

## Vibrational Study of ( $\eta^5$ -Cyclopentadienyl)metal Complexes

E. Diana,<sup>†</sup> R. Rossetti,<sup>†</sup> P. L. Stanghellini,<sup>\*,†</sup> and S. F. A. Kettle<sup>‡</sup>

Dipartimento di Chimica Inorganica, Chimica Fisica e Chimica dei Materiali, Università di Torino, via P. Giuria 7, 10125 Turin, Italy, and School of Chemical Sciences, University of East Anglia, Norwich NR4 7TJ, U.K.

Received May 16, 1996<sup>⊗</sup>

Raman and infrared spectral data on the vibrational modes of the  $M-(\eta^5-C_5H_5)$  unit have been collected and the fundamental assignments revisited. Complexes belonging to the metallocene series  $M(\eta^5-C_5H_5)$  and the cyclopentadienide salts  $[\eta^5-C_5H_5^-][M^+]$  have been studied, together with some monometallic  $(\eta^5-C_5H_5)ML_n$  and bimetallic  $(\eta^5-C_5H_5)_2M_2L_{2n}$  compounds. Comparison of the spectra shows a common vibrational pattern of the intraring modes, with minor variations in frequency and intensity, which allows the establishment of a vibrational fingerprint of general validity. Raman spectra give rise to a firm assignment of the skeletal metal–ring modes; a correlation is noted between the metal–ring stretch force constant and the metal–carbon distance. The approximate CH out-of-plane force constants vary considerably and presumably reflect different H–ring electrostatic repulsions.

### Introduction

The cyclopentadienyl ligand ( $C_5H_5$ , Cp) is one of the most common and versatile ligands in the field of organometallic chemistry. Starting with the ferrocene molecule, an enormous number of complexes with the  $M-Cp$  unit has been synthesized. In these the ligand may show, together with the most common  $\eta^5$  coordination, a variety of other bonding modes, such as  $\eta^1$ ,  $\eta^3$ ,  $\mu-\eta^2:\eta^3$ ,  $\mu-\eta^1:\eta^5$ , etc.<sup>1</sup>

The vibrational properties of the  $\eta^5$ -bonded cyclopentadienyl ligand have been the object of much interest. A few years after the synthesis of ferrocene, a fundamental paper appeared,<sup>2</sup> dealing with its vibrational spectra and assignments, and, despite subsequent discussions and comments, it substantially maintains its validity. Many vibrational data were reported in this period, mainly on ferrocene-like molecules, but also on other complexes with the  $Cp-M$  unit. The older data were reviewed by Fritz,<sup>3</sup> the most recent, by Aleksanyan.<sup>4</sup> Both authors attempted to correlate some vibrational features of the Cp ring with the type of metal–ligand bond: the classification of this bond into pure covalent, ionic, and an intermediate central- $\sigma$  bond dates back to these times. Recent interest in vibrational modes of  $Cp-M$  systems arises from theoretical force field calculations by molecular mechanics<sup>5</sup> and density functional methods.<sup>6</sup>

The scientific literature, mainly in the 1970s, contains a considerable number of papers dealing with the vibrational properties of more than one  $\eta^5$ -Cp complex. However, it is our opinion that a correlation between the different spectra is needed in an attempt to rationalize the different assignments and to establish, if possible, a common vibrational pattern for a Cp ring bonded to a metal atom. This is the main purpose of

the present paper. We have re-recorded and/or extended the spectra of several complexes and report the vibrational characteristic of others not previously studied. We have been led to return to the problem largely because we have obtained FT Raman (R) data on many of the species. While Raman data on  $\eta^5-C_5H_5$  species are available in the literature, they have shed little light on the problem outlined above. We believe that there is a reason for this, a reason which finds expression in the fact that, almost invariably, they have been presented in tabular form and not shown explicitly. In fact, the Raman spectra of  $\eta^5-C_5H_5$  species are difficult to obtain by conventional means. Many of the species are photochemically and/or thermally unstable, particularly in the presence of even a low concentration of oxygen. The use of a focused laser beam on a sample may well lead to the production of new species or decomposition products. By the same token, the species are often difficult to prepare in a sufficiently pure state to enable Raman spectra to be obtained free from the complication of fluorescence. Even a vestigial amount of fluorescence means that one is picking peaks off a broad background, with a consequently poor signal-to-noise ratio and uncertainty in peak position and even existence. Solution spectra are difficult to obtain for all of the above reasons combined with the need to achieve accurate optical alignments with a sample for which an inert atmosphere probably has to be maintained. The situation is quite different when FT Raman is used. Fluorescence and photolytic and thermal instability become minimal problems. Solution spectra can be obtained with relative ease. Not surprisingly, therefore, the availability of such data has proved key in enabling us to recognize vibrational spectroscopic features characteristic of the  $\eta^5-C_5H_5$  ligand which exhibit an essential transferability. In so doing, we have found that the infrared data on their own are not adequate to give these characteristics because they show a variability which can only be recognized and allowed for when reliable Raman data are available.

We have studied complexes belonging to the typically covalent  $Cp_2M$ , and to the formally ionic  $[Cp^-][M^+]$ , systems, as well as mononuclear  $CpM$  and binuclear  $(CpM)_2$  complexes, where other ligands, mainly CO, are bonded to the metal atom.

Tables 1 and 2 are helpful in providing guidelines for a better understanding of our vibrational analysis. Table 1 reports (see also ref 3) the schematic forms of the normal vibrations of the

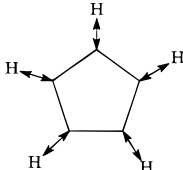
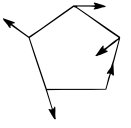
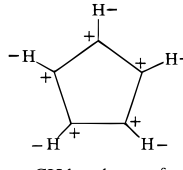
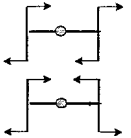
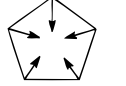
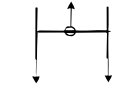
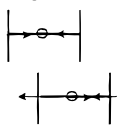
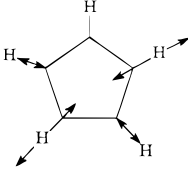
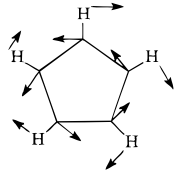
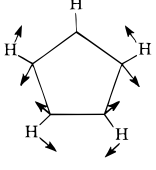
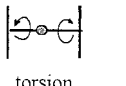
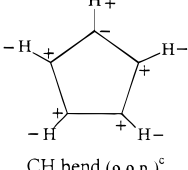
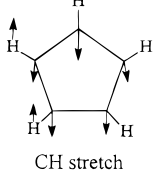
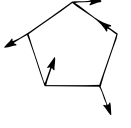
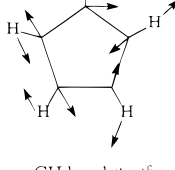
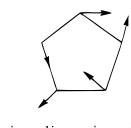
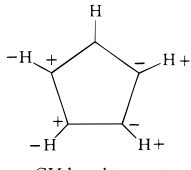
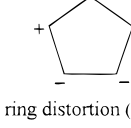
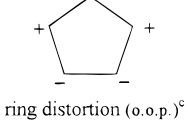
<sup>†</sup> Università di Torino.

<sup>‡</sup> University of East Anglia.

<sup>⊗</sup> Abstract published in *Advance ACS Abstracts*, December 1, 1996.

- (1) Elschenbroich, C.; Salzer, A. *Organometallics*, 2nd ed.; VCH: Weinheim, Germany, 1992; Chapter 15, pp 315–342.
- (2) Lippincott, E. R.; Nelson, R. D. *Spectrochim. Acta* **1958**, 307.
- (3) Fritz, H. P. *Adv. Organomet. Chem.* **1964**, 1, 239.
- (4) Aleksanyan, V. T. In *Vibrational spectra and structure*; Durig, J. R., Ed.; Elsevier: Amsterdam, 1982; Vol. 11, pp 107–167.
- (5) (a) Doman, T. N.; Landis, C. R.; Bosnich, B. *J. Am. Chem. Soc.* **1992**, 114, 7264. (b) Bosnich, B. *Chem. Soc. Rev.* **1994**, 387. (c) Doman, T. N.; Hollis, T. K.; Bosnich, B. *J. Am. Chem. Soc.* **1995**, 117, 1352.
- (6) Bérces, A.; Ziegler, T.; Fan, L. *J. Phys. Chem.* **1994**, 98, 1584.

**Table 1.** Description of the Fundamental Modes of Vibration of  $\text{Cp}_2\text{M}$  Molecules

mode			mode		mode		mode		
symmetry <sup>b</sup>	number	description <sup>a</sup>	number	symmetry <sup>b</sup>	symmetry <sup>b</sup>	number	description <sup>a</sup>	number	symmetry <sup>b</sup>
$A_{1g}$	1	 CH stretch	8	$A_{2u}$	$E_{1g}$	15		20	$E_{1u}$
	2	 CH bend (o.o.p.) <sup>c</sup>	9			16	 CC stretch	21	
	3	 ring breath	10			22	 ring tilt	22	
	4	 M-ring stretch	11			23	 ring M-ring bend	29	$E_{2u}$
$A_{2g}$	7	 CH bend (i.p.)	5	$A_{1u}$		24	 CH stretch	30	
		 torsion	6			25	 CH bend (o.o.p.) <sup>c</sup>	31	
$E_{1g}$	12	 CH stretch	17	$E_{1u}$		26	 CH bend (o.o.p.) <sup>c</sup>	32	
	13	 CH bend (i.p.) <sup>c</sup>	18			27	 CC stretch	33	
	14	 CH bend (o.o.p.)	19			28	 ring distortion (i.p.) <sup>c</sup>	34	
							 ring distortion (o.o.p.) <sup>c</sup>		

<sup>a</sup> The description shows schematically the main component of the mode referred to a single  $\text{C}_5\text{H}_5$  ring. The modes on the left column represent the in-phase coupling; those on the right column, the out-of-phase coupling. <sup>b</sup> The symmetry corresponds to the  $D_{5d}$  point group. <sup>c</sup> The in-phase (i.p. or  $\delta$ ) and the out-of-phase (o.o.p. or  $\gamma$ ) notation refers to the  $\text{C}_5\text{H}_5$  plane.

$\text{C}_5\text{H}_5$  group (only the main component of each vibration is given), together with the in-phase and out-of-phase coupling of these modes for a ferrocene-like molecule of  $D_{5d}$  symmetry.

Also indicated is the character, in terms of internal coordinate, of the main component. The numbering of the modes are those already reported<sup>2</sup> and are those generally used. Table 2

**Table 2.** Correlation between the Modes of Cp<sub>2</sub>M, CpM, and [Cp<sup>-</sup>]

character	Cp <sub>2</sub> M mode	CpM (C <sub>5v</sub> )			[Cp <sup>-</sup> ] (D <sub>5h</sub> )		
		mode	symmetry	activity	mode	symmetry	activity
ν(C-H)	1 and 8	1'	a <sub>1</sub>	IR R	1''	a <sub>1</sub> '	R
	12 and 17	7'	e <sub>1</sub>	IR R	5''	e <sub>1</sub> '	IR
	23 and 29	13'	e <sub>2</sub>	R	9''	e <sub>2</sub> '	R
ν(C-C)	3 and 10	3'	a <sub>1</sub>	IR R	2''	a <sub>1</sub> '	R
	15 and 20	10'	e <sub>1</sub>	IR R	7''	e <sub>1</sub> '	IR
	26 and 32	16'	e <sub>2</sub>	R	11''	e <sub>2</sub> '	R
δ(C-H)	5 and 7	5'	a <sub>2</sub>	inact	3''	a <sub>2</sub> '	inact
	13 and 18	8'	e <sub>1</sub>	IR R	6''	e <sub>1</sub> '	IR
	24 and 30	14'	e <sub>2</sub>	R	10''	e <sub>2</sub> '	R
γ(C-H)	2 and 9	2'	a <sub>1</sub>	IR R	4''	a <sub>2</sub> ''	IR
	14 and 19	9'	e <sub>1</sub>	IR R	8''	e <sub>1</sub> ''	R
	25 and 31	15'	e <sub>2</sub>	R	13''	e <sub>2</sub> ''	inact
δ(C-C-C)	27 and 33	17'	e <sub>2</sub>	R	12''	e <sub>2</sub> '	R
	28 and 34	18'	e <sub>2</sub>	R	14''	e <sub>2</sub> ''	inact
	ν(M-Cp)	4 and 11	4'	a <sub>1</sub>	IR R		
ring tilt	16 and 21	11'	e <sub>1</sub>	IR R			
δ(Cp-M-Cp)	22	12'	e <sub>1</sub>	IR R			
ring torsion	6	6'	a <sub>2</sub>	inact			

correlates the modes of Table 1 with those of a CpM fragment under local C<sub>5v</sub> symmetry and with those of the [C<sub>5</sub>H<sub>5</sub>]<sup>-</sup> anion, of D<sub>5h</sub> symmetry. The numbering of the modes of the CpM fragment in Table 2 cannot be anything but arbitrary; the other modes of the molecule are not included.

## Experimental Section

**General Procedure.** All of the manipulations of air-sensitive compounds were performed using either Schlenk procedures or a glovebox filled with dry argon. All of the solvents employed were degassed by repeated cycles of freeze-pumping under a vacuum. Tetrahydrofuran (THF) was distilled from sodium-benzophenone.

**Synthesis of the Complexes.** Many of complexes studied are commercial products. Cp<sub>2</sub>V, Cp<sub>2</sub>Cr, Cp<sub>2</sub>Fe, Cp<sub>2</sub>Co, CpTi, CpMn(CO)<sub>3</sub> (Aldrich), and Cp<sub>2</sub>Ni (Strem) were purified by sublimation at reduced pressure. [CpFe(CO)<sub>2</sub>]<sub>2</sub>, [CpMo(CO)<sub>3</sub>]<sub>2</sub>, [CpW(CO)<sub>3</sub>]<sub>2</sub>, CpLi (Aldrich), and [CpNi(CO)]<sub>2</sub> (Chemical Pressure) were purified by crystallization. The cis- and trans-isomers of [CpFe(CO)<sub>2</sub>]<sub>2</sub>, were isolated by the reported procedure.<sup>7</sup> All of the other complexes were prepared according to literature methods: Cp<sub>2</sub>Mg,<sup>8</sup> Cp<sub>2</sub>Mn,<sup>9</sup> [Cp<sub>2</sub>Fe<sup>+</sup>][I<sub>3</sub><sup>-</sup>],<sup>10</sup> [Cp<sub>2</sub>Co<sup>+</sup>][Br<sub>3</sub><sup>-</sup>],<sup>11</sup> CpFe(CO)<sub>2</sub>Cl,<sup>12</sup> CpFe(CO)<sub>2</sub>Br,<sup>13</sup> CpFe(CO)<sub>2</sub>I,<sup>14</sup> and CpRe(CO)<sub>3</sub>.<sup>15</sup>

The starting reagents C<sub>10</sub>H<sub>12</sub>, Na, K, Mg, MnBr<sub>2</sub>, RuCl<sub>3</sub>, and Br<sub>2</sub>, Re(CO)<sub>5</sub>Cl were purchased from Aldrich. The common reactants and solvents were purchased from Carlo Erba. CpNa and CpK were synthesized by reaction of freshly distilled C<sub>3</sub>H<sub>6</sub> with sodium and potassium sand in THF.

**Spectroscopic Measurements.** The mid-infrared spectra of the air-stable complexes were recorded as CsI pellets on a Perkin-Elmer IR grating spectrophotometer (Model 580B) and the spectral data obtained with the PE580 software provided. The spectra of CpM (M = Li, Na, K) were recorded as nujol dispersions. The spectra of air-sensitive metallocenes were obtained by high-vacuum sublimation onto a CsI pellet cooled with liquid N<sub>2</sub> and recorded on a Perkin-Elmer FTIR (Model 2000). All the far-IR spectra were recorded as PET pellets on a Bruker spectrophotometer (Model 113).

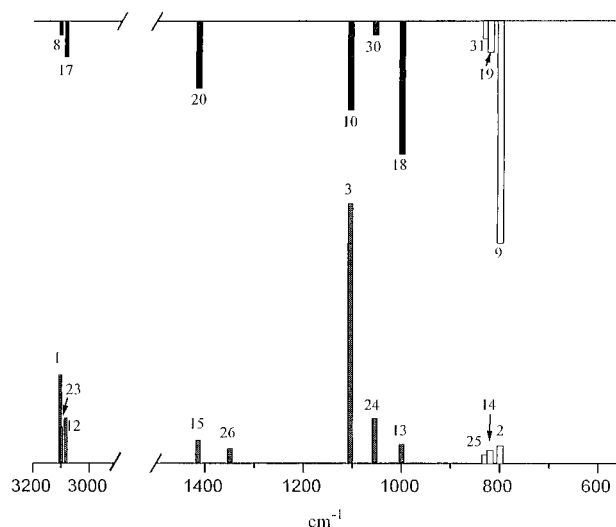


**Figure 1.** Schematic representation of the main vibrational features of the solid state infrared (upper) and Raman (lower) spectra of metallocene complexes. Open bars are the C-H out-of-plane bending modes. The mode numbers are those in Table 1.

The samples for the Raman spectra were prepared by sealing crystals of the complexes in a glass capillary under argon. The extremely air- and moisture-sensitive Cp<sub>2</sub>Mn required sublimation of the sample in a capillary sealed under high vacuum. The spectra were run on a Bruker RFS 100, with Nd<sup>3+</sup>:YAG Laser and Ge-diode detector (laser power between 20 and 100 mW, resolution usually 4 cm<sup>-1</sup>). The white light correction did not give rise to significant changes in the spectra, except, in some cases, to a small decrease of the intensity of the bands around 3000 cm<sup>-1</sup>.

## Results

In the following description we have preferred to treat the intraring modes (i.e., the CH and CC stretching and the CH in-plane and out-of-plane bending) separately from the interring or skeletal modes, which involve the metal atom or other ligands. Although this separation is somewhat arbitrary (e.g., the ring deformation, an intraring mode, has also metal-stretching character and so has sometimes been considered as an interring mode when this aspect was relevant), it is of considerable practical use, as will immediately be evident.

**(1) Intraring Modes. (A) Metallocenes Cp<sub>2</sub>M.** The schematic diagram in Figure 1 illustrates the infrared and Raman spectra of metallocenes in the solid state in the spectral region of the intraring vibrations. The patterns shown summarize the

(7) Bryan, R. F.; Greene, P. T.; Newlands, M. J.; Field, D. S. *J. Chem. Soc. A* **1970**, 3068.

(8) Barber, W. A. *Inorg. Synth.* **1960**, 6, 11.

(9) Wilkinson, G.; Cotton, F. A.; Birmingham, J. M. *J. Inorg. Nucl. Chem.* **1956**, 2, 95.

(10) Hendrickson, D. N.; Sohn, Y. S.; Gray, H. B. *Inorg. Chem.* **1971**, 10, 1559.

(11) Hartley, D.; Ware, M. J. *J. Chem. Soc. A* **1969**, 138.

(12) Piper, T. S.; Cotton, F. A.; Wilkinson, G. *J. Inorg. Nucl. Chem.* **1955**, 1, 165.

(13) Hallam, B. F.; Pauson, P. L. *J. Chem. Soc. A* **1956**, 3030.

(14) King, R. B.; Stone, F. G. A. *Inorg. Synth.* **1963**, 7, 110.

(15) Fisher, E. O.; Fellman, W. *J. Organomet. Chem.* **1963**, 1, 191.

spectra of complexes with  $M = \text{Mg, V, Cr, Mn, Fe, Fe}^+, \text{Co, Co}^+, \text{and Ni}$ . These spectral patterns can be considered vibrational "finger prints" of  $\text{Cp}_2\text{M}$  complexes, as both the frequencies and the relevant intensities of the IR and Raman bands vary over quite narrow ranges, except for those corresponding to the CH out-of-plane bending modes.

The following comments are important.

(i) The frequencies of a symmetric mode (Raman) and of the corresponding antisymmetric mode (infrared) of the internal vibrations of the two rings are nearly identical:<sup>16</sup> this confirms that the coupling between the two rings is negligible for all of the complexes. The small differences observed could well result from solid state effects.

(ii) The common fingerprint pattern resolves some ambiguities or contradictory assignments reported in the literature (see, in particular, the case of  $\text{Cp}_2\text{Mg}$ ).<sup>15,17</sup> So, it shed light on a problem concerning modes 24 and 30, first assigned to the bands at ca.  $1190\text{--}1210\text{ cm}^{-1}$ <sup>19</sup> and subsequently reassigned to the absorption at ca.  $1050\text{ cm}^{-1}$ , on the basis of experimental intensities<sup>20</sup> and theoretical calculations.<sup>5a,6</sup> The fingerprint also supports the reassignment. As a consequence of this change, modes 25 and 31 (C–H out-of-plane deformations), previously reported as being at ca.  $1050\text{ cm}^{-1}$ , contribute, we believe, to the band pattern between  $750\text{ and }900\text{ cm}^{-1}$ , a range where the modes of species with similar parentage occur.

(iii) All thirteen Raman-active intraring modes usually appear in the spectrum, which is dominated by a very strong band at ca.  $1100\text{ cm}^{-1}$  and by another at ca.  $3100\text{ cm}^{-1}$ , assigned to the totally symmetric modes 3 and 1, respectively. In a few cases, e.g.,  $\text{Cp}_2\text{Mg}$ , some modes of  $e_{1g}$  (13 and 15) or  $e_{2g}$  (27 and 28) symmetry have an intensity too low to be clearly seen above the background.

(iv) The bands belonging to the eight infrared-active intraring modes are usually all evident in the spectrum, but their relevant intensities are more variable than those of the Raman-allowed modes; so the infrared spectrum shown in Figure 1 should be taken as indicative only, as far as the intensities are concerned. However, the most prominent bands correspond to modes 9, 10, 18, and 20. Sometimes, some formally infrared-inactive modes, such as the  $e_{2u}$  29 and 30, appear with low intensity, probably because of crystal effects. Their assignment is based on a comparison with their Raman-active  $e_{2g}$  counterparts (23 and 24). A weak band often appears at ca.  $1250\text{ cm}^{-1}$  and is assigned to the  $a_{1u}$  IR-inactive mode (5), which is without a Raman-active counterpart. Their assignment is supported by theoretical calculations.<sup>5a,6</sup> It is noteworthy that among the intraring modes the C–H out-of-plane bending vibrations are the only ones which show significant variation in their frequencies (see later).

(v) The spectral anomaly presented by manganocene in the C–H stretching region has to be recognized. The Raman spectrum shows four strong bands of ca. equal intensity at  $3111, 3099, 3065, \text{ and } 3046\text{ cm}^{-1}$ ; the infrared spectrum, two medium bands and one weak band at  $3085, 3075, \text{ and } 3041\text{ cm}^{-1}$ , respectively. This pattern clearly does not exactly conform with the fingerprint scheme. The discrepancy can be associated with the anomalous crystal structure of manganocene—it has a zigzag

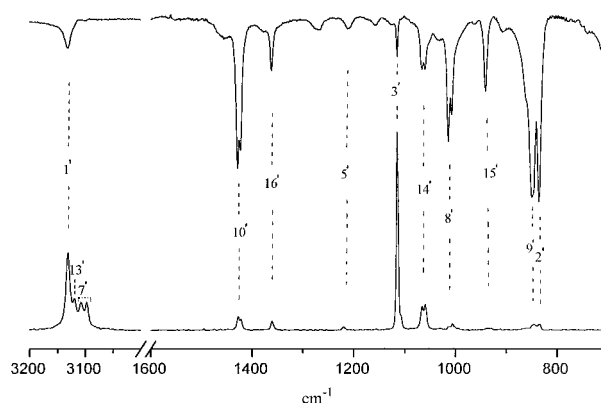


Figure 2. Infrared (upper) and Raman (lower) spectra of  $\text{CpMn}(\text{CO})_3$  in the solid state.

$\text{Cp-Mn}(\text{Cp})\text{-Cp-Mn}(\text{Cp})\text{-...}$  chain, with terminal  $\eta^5\text{-C}_5\text{H}_5$  and bridging  $\eta^2:\eta^3\text{-C}_5\text{H}_5$  rings.<sup>21</sup> It is remarkable that this structural difference affects the  $\nu(\text{CH})$  pattern only, the remainder of the spectra being very close to the general behavior.

**(B) Complexes of the Type  $\text{CpML}_n$ .** The complexes we have studied are  $\text{CpM}(\text{CO})_3$  ( $M = \text{Mn, Re}$ ) and  $\text{CpFe}(\text{CO})_2\text{X}$  ( $X = \text{Cl, Br, I}$ ). The molecular symmetries are different and generally low, but the fragment  $\text{CpM}$  can be treated on the basis of the local  $C_{5v}$  symmetry. This assumption is usually accepted<sup>22–24</sup> and implies the exclusion of any coupling between the vibrations of the  $\text{CpM}$  fragment and of the  $L_n$  fragment. This is clearly unacceptable as far as skeletal modes are concerned, but it may be valid for the intraring vibrations, which, as we have seen, are essentially uncoupled, even between two identical Cp rings.

Figure 2 shows model infrared and Raman spectra of  $\text{CpMn}(\text{CO})_3$ . Two important regions for intraring modes are shown, that between  $3200\text{ and }3000\text{ cm}^{-1}$  and that between  $1500\text{ and }600\text{ cm}^{-1}$ . Other regions, showing the very strong CO modes, are excluded for clarity of presentation.

It is evident that the pattern of intraring bands is very close to that of the general scheme reported in Figure 1. This is particularly clear for the Raman spectra, the infrared spectra sometimes showing an unexpectedly low intensity in some allowed modes. The low molecular and/or crystal symmetry may be responsible for minor but significant modifications. So, the spectra show a splitting of the majority of the  $e_1$  modes. However, on the basis of the fingerprint scheme and of the mode correlation (Table 2), the assignments shown in the figure are straightforward.

**(C) Complexes of the type  $\text{Cp}_2\text{M}_2(\text{CO})_n$ .** The complexes studied,  $\text{Cp}_2\text{Ni}_2(\text{CO})_2$ ,  $\text{Cp}_2\text{Fe}_2(\text{CO})_4$  (cis and trans forms), and  $\text{Cp}_2\text{M}_2(\text{CO})_6$  ( $M = \text{Mo, W}$ ), have been selected on the basis of a common skeletal  $\text{Cp-M-M-Cp}$  structure, as illustrated in the Chart 1.

The central region of the spectra is reported in Figure 3 (Raman) and Figure 4 (infrared). The spectral patterns are apparently more complicated than the fingerprint scheme, but the basic features are easily interpreted on this basis, as indicated by the markers at the head of the figures, markers which refer to Table 2.

The multiplicity of the bands arises from the splitting of the local  $e_1$  and  $e_2$  modes, presumably because of the lower

(16) Tables with the complete list of the frequency values of all of the complexes are included in the Supporting Information.

(17) Lippincott, E. R.; Xavier, J.; Steele, D. *J. Am. Chem. Soc.* **1961**, *83*, 2262.

(18) Aleksanyan, V. T.; Garbuzova, I. A.; Gavrilenko, V. V.; Zakharkin, L. I. *J. Organomet. Chem.* **1977**, *129*, 139.

(19) Bodenheimer, J. S.; Low, W. *Spectrochim. Acta* **1973**, *29A*, 1733.

(20) Aleksanyan, V. T.; Lokshin, B. V.; Borison, G. K.; Devyatykh, G. G.; Smirnov, A. S.; Nazarova, R. V.; Koningstein, J. A.; Gächter, B. F. *J. Organomet. Chem.* **1977**, *124*, 293.

(21) Weiss, E.; Buender, W. *Z. Naturforsch.* **1978**, *33B*, 1235.

(22) Adams, D. M.; Squire, A. *J. Organomet. Chem.* **1973**, *63*, 381.

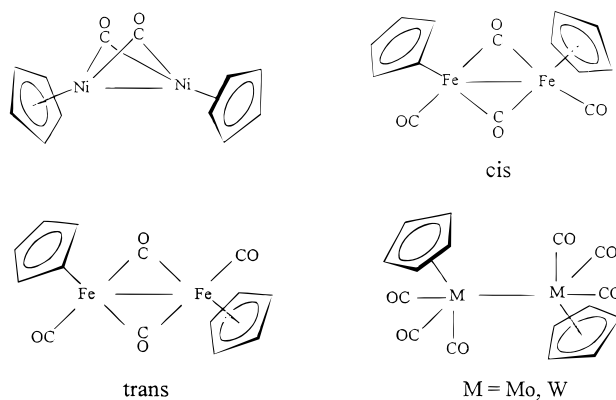
(23) Lokshin, B. V.; Klemenkova, Z. S.; Makarov, Y. V. *Spectrochim. Acta* **1972**, *28A*, 2209.

(24) Hyams, I. J.; Bailey, R. T.; Lippincott, E. R. *Spectrochim. Acta* **1967**, *23A*, 273.



**Figure 3.** Raman spectra in the 700–1500  $\text{cm}^{-1}$  region of (a)  $\text{Cp}_2\text{Fe}_2(\text{CO})_4$  trans isomer, (b)  $\text{Cp}_2\text{Fe}_2(\text{CO})_4$  cis isomer, (c)  $\text{Cp}_2\text{Mo}_2(\text{CO})_6$ , and (d)  $\text{Cp}_2\text{W}_2(\text{CO})_6$ , (e)  $\text{Cp}_2\text{Ni}_2(\text{CO})_2$ . The broad absorption in c at ca. 800  $\text{cm}^{-1}$  is due to fluorescence.

### Chart 1



symmetry in the crystals. The complexity of the pattern of the CH out-of-plane bending modes for  $\text{Cp}_2\text{Ni}_2(\text{CO})_2$  and for the cis form of  $\text{Cp}_2\text{Fe}_2(\text{CO})_4$  suggests a possible coupling between these modes and the bridging CO bending modes. The behavior of the  $\nu(\text{C}-\text{H})$  modes, illustrated by the Raman spectra in Figure 5 (the corresponding infrared absorption are weak and not so informative), may well be explained by intermolecular coupling effects in the crystals. The number of bands and their relevant intensities for the cis isomer of  $\text{Cp}_2\text{Fe}_2(\text{CO})_4$  and for the  $\text{Cp}_2\text{M}_2(\text{CO})_6$  compounds do not accord either with that of a unique Cp–M unit (Figure 2) or with that of two uncoupled Cp rings (Figure 1). The number is not explicable in terms of a simple site-symmetry splitting of the  $e_1$  and  $e_2$  modes, either.

**(D) Complexes of the Type CpM.** The above complexes, where  $\text{M}$  = alkali metals or Tl, have traditionally been considered to be ionic complexes  $[\text{Cp}^-][\text{M}^+]$ .<sup>3,4</sup> If this is so, their spectra should simply be the spectra of the  $[\text{C}_5\text{H}_5^-]$  with  $D_{5h}$  symmetry and should consist of seven Raman and four

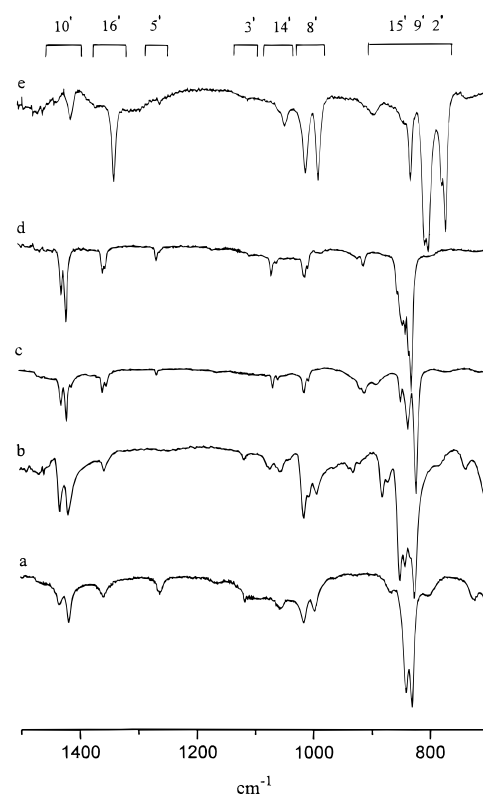


**Figure 4.** Infrared spectra in the 700–1500  $\text{cm}^{-1}$  region of (a)  $\text{Cp}_2\text{Fe}_2(\text{CO})_4$  trans isomer, (b)  $\text{Cp}_2\text{Fe}_2(\text{CO})_4$  cis isomer, (c)  $\text{Cp}_2\text{Mo}_2(\text{CO})_6$ , (d)  $\text{Cp}_2\text{W}_2(\text{CO})_6$ , and (e)  $\text{Cp}_2\text{Ni}_2(\text{CO})_2$ .

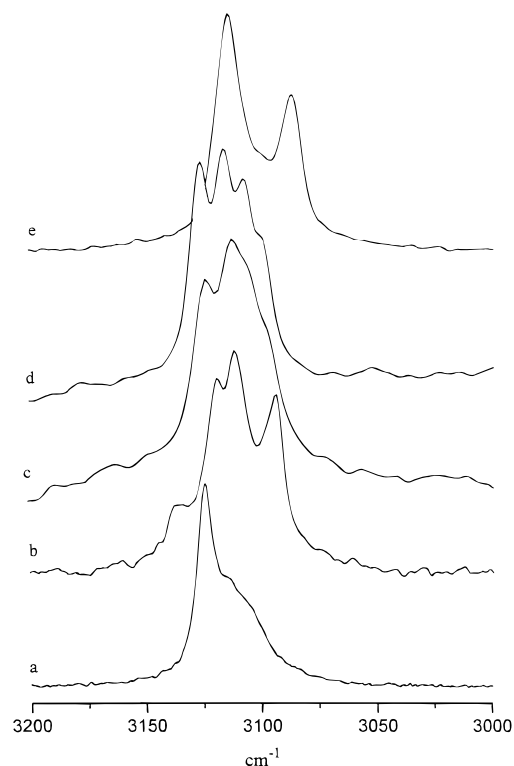


**Figure 5.** Raman spectra in the C–H stretching region of (a)  $\text{Cp}_2\text{Fe}_2(\text{CO})_4$  trans isomer, (b)  $\text{Cp}_2\text{Fe}_2(\text{CO})_4$  cis isomer, (c)  $\text{Cp}_2\text{Mo}_2(\text{CO})_6$ , (d)  $\text{Cp}_2\text{W}_2(\text{CO})_6$ , and (e)  $\text{Cp}_2\text{Ni}_2(\text{CO})_2$ .

infrared bands (see Table 2). The basic pattern of the spectra of the complexes with Li, K, and Tl fulfils this expectation and can be interpreted by the fingerprint scheme, with the obvious simplifications. However, the ionic model leads us to expect nearly coincident spectra, which are of course the spectra of

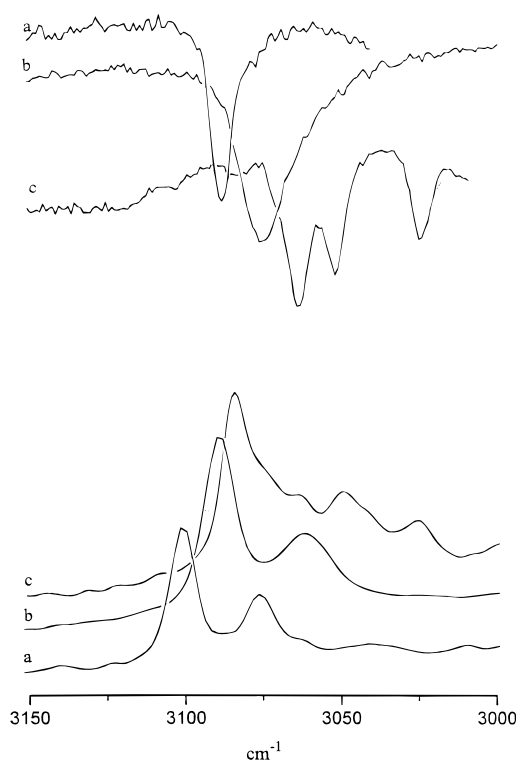


**Figure 6.** Infrared (upper) and Raman (lower) spectra in the C–H stretching region of (a) CpLi, (b) CpTl, and (c) CpK.

$[\text{C}_5\text{H}_5^-]$ . In fact,  $\Delta\nu$  values between the same mode for different complexes are not negligible, often exceeding  $10\text{ cm}^{-1}$ . Moreover, additional features can be evident. For CpLi and CpTl the  $\nu(\text{CH})$  pattern is that expected, i.e., two Raman and one infrared features, but is very different for CpK, where the presumed  $e_1$  mode has both split and acquired Raman intensity. Similarly, the  $e_2$  mode is infrared-active (Figure 6). As C–H stretching vibrations are sensitive to structural deformations and to crystal effects, the data indicate for CpK either a distortion of the ring or strong interring coupling. These interpretations are supported by the observation of an unique feature at  $3050\text{ cm}^{-1}$  in the IR spectrum in THF solution. The intermediate region ( $600\text{--}1500\text{ cm}^{-1}$ ) shows the expected  $\nu(\text{C–C})$ ,  $\delta(\text{C–H})$ , and  $\gamma(\text{C–H})$  modes, with the correct R or IR activity, but also an unexpected IR absorption of mode  $8''$  for K and Tl. For the latter there is also a medium Raman band at  $1206\text{ cm}^{-1}$ , which can be tentatively assigned to mode  $3''$ , on the basis of calculations available for  $[\text{Cp}^-]$  and for CpLi.<sup>6</sup> These departures from the simple model indicate that metal–ring interactions are nonzero, that, not surprisingly, the pure ionic model is a simplification.

#### (2) Interring or Skeletal Modes. (A) Metallocenes $\text{Cp}_2\text{M}$ .

The interring or skeletal modes include the symmetric and antisymmetric ring–metal stretching (modes 4 and 11), the metal–ring tilting (modes 16 and 21), and the ring–metal–ring bending (mode 22). The ring deformation modes also have some metal–ring stretching character. The metal–ring stretching modes and the tilting modes are significantly coupled, the antisymmetric component having a higher frequency than the corresponding symmetric mode ( $\nu_{11} > \nu_4$  and  $\nu_{21} > \nu_{16}$ ). The ring tilt vibrations lie at a higher frequency than the metal–ring stretching vibrations, for all except nickelocene, where the order is reversed (the unique assignment is based on the low Raman intensity and the splitting of the tilt modes: see also ref 25).

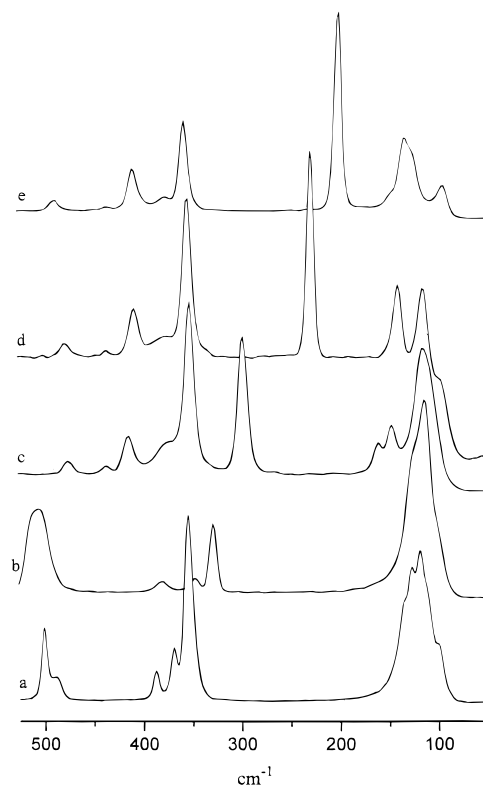


**Figure 7.** Raman spectra in the  $50\text{--}500\text{ cm}^{-1}$  region of (a) CpMn( $\text{CO}$ )<sub>3</sub>, (b) CpRe( $\text{CO}$ )<sub>3</sub>, (c) CpFeCl( $\text{CO}$ )<sub>2</sub>, (d) CpFeBr( $\text{CO}$ )<sub>2</sub>, and (e) CpFeI( $\text{CO}$ )<sub>2</sub>.

The relative intensities of the bands are very variable, the only common feature being the high Raman intensity of the symmetric metal–ring stretching; the other Raman-allowed mode gives rise to a medium-strong band in Cp<sub>2</sub>V, Cp<sub>2</sub>Mn, Cp<sub>2</sub>Fe,  $[\text{Cp}_2\text{Co}^+]$ , and Cp<sub>2</sub>Ni but to a weak and broad band in Cp<sub>2</sub>Mg, Cp<sub>2</sub>Cr,  $[\text{Cp}_2\text{Fe}^+]$ , and Cp<sub>2</sub>Co. The infrared-allowed modes 11 and 21 appear as medium bands in Cp<sub>2</sub>Mg, Cp<sub>2</sub>V, Cp<sub>2</sub>Fe, and  $[\text{Cp}_2\text{Co}^+]$  and as weak bands in Cp<sub>2</sub>Cr,  $[\text{Cp}_2\text{Fe}^+]$ , Cp<sub>2</sub>Co, and Cp<sub>2</sub>Ni. The bending mode is weak and often cannot be assigned with confidence. All of the evidence indicates that there is no vibrational fingerprint of general validity for these compounds in this region.

**(B) Complexes of the type  $\text{CpML}_n$ .** For these species, the assignment of the skeletal modes could be complicated by coupling with modes involving other ligands, CO groups in particular. Nonetheless, a close inspection of Figure 7, showing the Raman spectra of CpMn( $\text{CO}$ )<sub>3</sub>, of CpRe( $\text{CO}$ )<sub>3</sub>, and of CpFe( $\text{CO}$ )<sub>2</sub>X (X = Cl, Br, I) in the  $50\text{--}500\text{ cm}^{-1}$  region, shows a surprising similarity between different spectra, notwithstanding the differences of metal, surrounding ligands, and symmetry of the complex. The spectra all show a strong band around  $350\text{ cm}^{-1}$ , together with two medium-weak bands at somewhat higher frequencies. The frequency and intensity values exclude assignment to M–C–O modes but point to metal–ring stretching modes, which are formally three,  $a_1$ ,  $e_1$ , and  $e_2$ , on the basis of a local  $C_{5v}$  symmetry ( $4'$ ,  $11'$ , and  $18'$  in Table 2, respectively). Of these,  $e_1$  mode can be regarded as a ring tilt relative to the local  $C_5$  axis and the  $e_2$  mode has out-of-plane ring deformation character. The symmetric stretch  $a_1$  ( $4'$ ) for CpM( $\text{CO}$ )<sub>3</sub> complexes is surely at  $353$  and at  $327\text{ cm}^{-1}$  when M = Mn<sup>22,24,26</sup> or Re,<sup>23</sup> respectively. A similar assignment is

(25) Chhor, K.; Lucazeau, G.; Sourisseau, C. *J. Raman Spectrosc.* **1981**, *11*, 183.

(26) Lokshin, B. V.; Rusach, E. B.; Setkina, V. N.; Pyshnograeva, N. I. *J. Organomet. Chem.* **1974**, *77*, 69.

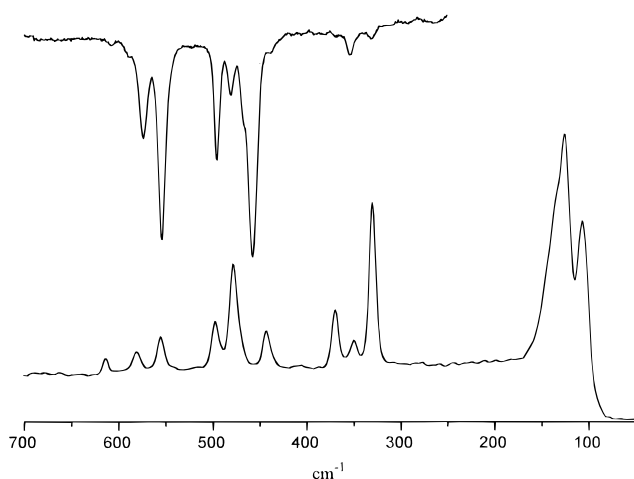


**Figure 8.** Infrared (upper) and Raman (lower) spectra of  $\text{Cp}_2\text{W}_2(\text{CO})_6$  in the  $100\text{--}700\text{ cm}^{-1}$  region.

straightforward for the other complexes. The other two bands, close to the strong totally symmetric ones, can be attributed to modes  $11'$  and  $18'$ , the intermediate being probably  $e_1$ , because of the essentially coincidence with a corresponding infrared absorption. Some marginally different assignments<sup>22,24,26</sup> may be ruled out, because of the general pattern similarity, a pattern, interestingly, also found in the spectra of (pyrrolyl) $\text{Mn}(\text{CO})_3$ .<sup>26</sup> A strong band in the  $\text{CpFe}(\text{CO})_2\text{X}$  spectra, moving toward lower frequency as the mass of X increases, is clearly the  $\nu(\text{Fe-X})$  mode. The large unresolved envelope below  $150\text{ cm}^{-1}$  presumably includes, among others, the Cp-M-L bending vibrations.

**(C) Complexes of the type  $\text{Cp}_2\text{M}_2(\text{CO})_n$ .** The analysis of the skeletal modes appearing in the low-frequency ( $<450\text{ cm}^{-1}$ ) region is not immediate but can be helped by a comparison of the infrared and the Raman spectra of different complexes. We begin with the analysis of the spectra of  $\text{Cp}_2\text{W}_2(\text{CO})_6$ , which appears to be the simplest (Figure 8), and attempt an acceptable interpretation of the skeletal modes. The region between  $650$  and  $400\text{ cm}^{-1}$  seems neatly separated from the remainder and shows bands undoubtedly belonging to W-C-O modes. On the basis of idealized  $C_{2h}$  molecular symmetry,<sup>27</sup> nine infrared- and nine Raman-active modes are expected without coincidences and at least seven infrared bands are observed, with no coincidences with the seven Raman bands. At lower frequency, the pattern between  $400$  and  $300\text{ cm}^{-1}$  is very close to that of  $\text{CpML}_n$  complexes, and its interpretation is similarly straightforward. Thus, the strong Raman band at  $330\text{ cm}^{-1}$  (corresponding to a weak infrared band at  $331\text{ cm}^{-1}$ ) is assigned to the symmetric  $\nu(\text{Cp-W})$  mode. A medium-weak band at  $354/350\text{ cm}^{-1}$  appearing in both infrared and Raman is clearly the  $e_1$  ring tilt mode. The medium-strong Raman band (without infrared counterpart) at  $370\text{ cm}^{-1}$  must be the  $e_2$  ring deformation mode. The simple pattern with appropriate IR/R coincidence suggests that a local  $C_{5v}$  symmetry is operative, without coupling between the Cp-W units.

The spectral pattern of  $\text{Cp}_2\text{Mo}_2(\text{CO})_6$  is almost superimposable on that of the W analogue. The Cp-Mo modes have IR/R frequencies at  $339\text{ w}/335\text{ s cm}^{-1}$  ( $a_1$ ), at ca.  $352\text{ w}/345\text{ m,sh cm}^{-1}$  ( $e_1$ ), and at  $-/369\text{ m cm}^{-1}$  ( $e_2$ ).

In these spectra, the  $\nu(\text{M-M})$  band probably lies among the broad and strong Raman absorptions centred at ca.  $125\text{ cm}^{-1}$  (W) and at  $118\text{ cm}^{-1}$  (Mo). The long M-M distances<sup>27</sup> suggest low-frequency values. In contrast, the complex  $\text{Cp}_2\text{Mo}_2(\text{CO})_4$ ,

with a shorter—formally triple—Mo-Mo bond shows a very strong Raman absorption at  $227\text{ cm}^{-1}$ , assigned to the Mo-Mo stretching mode.

Moving to the  $\text{Cp}_2\text{Fe}_2(\text{CO})_4$  isomers, some additional complications arise. The spectral pattern is, more or less, similar. The bands above  $430\text{ cm}^{-1}$  are assigned to the Fe-C-O modes, as indicated by their pattern of strong infrared and weak Raman bands. A previous assignment,<sup>28</sup> based on infrared spectra only, does not seem reliable. The pattern around  $400\text{ cm}^{-1}$  is very close to that of  $\text{Cp}_2\text{W}_2(\text{CO})_6$ , and the same assignment follows. The strong Raman band at  $228\text{ cm}^{-1}$  is clearly the  $\nu(\text{Fe-Fe})$  mode. However, closer observation suggests that the problem is not so simple. Thus, the Raman and the infrared frequencies do not always coincide, and the  $\Delta\nu$  is too great ( $8\text{--}10\text{ cm}^{-1}$ ) to be ascribed to sampling or instrumental error. Moreover, a medium Raman band at  $267\text{ cm}^{-1}$  and a medium-weak infrared band at  $247\text{ cm}^{-1}$  are without assignment in the simple model. Two possible general explanations can be suggested: intramolecular coupling between the two Cp-Fe units in the molecule or intermolecular coupling between the two molecules in the unit cell.<sup>29</sup> The dilemma is resolved by the solution spectra. Despite the strong solvent backgrounds, careful subtraction reveals Raman bands at  $351$  ( $\text{CH}_3\text{CN}$ ) or  $350\text{ cm}^{-1}$  ( $\text{CCl}_4$ ) with a corresponding band at  $348\text{ cm}^{-1}$  ( $\text{CH}_2\text{Cl}_2$ ). These are unambiguously the  $a_1$  mode. There is an infrared band at  $387\text{ cm}^{-1}$ , without Raman counterpart, which must be the  $e_1$  mode. Finally, there is a Raman only band at  $410$  ( $\text{CH}_3\text{CN}$ ) or at  $406\text{ cm}^{-1}$  ( $\text{CCl}_4$ ), clearly the  $e_2$  mode.  $\nu(\text{Fe-Fe})$  at  $228\text{ cm}^{-1}$  (Raman,  $\text{CH}_3\text{CN}$ ) is also clear; all other features are absent. So, the intramolecular coupling explanation is excluded, and the interpretation of the additional features in the solid state must lie in the intermolecular coupling.

This background makes easier the interpretation of the complex spectra of  $\text{Cp}_2\text{Ni}_2(\text{CO})_2$ . The Raman spectrum is dominated by two strong bands at  $390$  and  $199\text{ cm}^{-1}$ , straightforwardly assigned to the  $\nu(\text{Cp-Ni})$  and  $\nu(\text{Ni-Ni})$   $a_1$  modes, respectively. The latter band is split at higher resolution ( $2\text{ cm}^{-1}$ ) into two equally intense absorptions at  $195$  and  $201\text{ cm}^{-1}$ , well-accounted for by the two independent molecules (with different Ni-Ni bonding distances) in the unit cell.<sup>30</sup> The spectral pattern also shows the unusual pattern of the other  $\nu(\text{Cp-Ni})$  modes, of  $e_1$  and  $e_2$  symmetries, having lower frequencies than the  $a_1$  mode, with the same sequence observed, for instance, in  $\text{Cp}_2\text{Ni}$  (see also ref 25). Their frequencies appear to be in the order  $e_1 > e_2$ , based on the relevant Raman and infrared intensities. As in the previous case, the significant  $\Delta\nu$  value between corresponding IR and Raman bands may be ascribed to intermolecular coupling and not to intramolecular coupling. The solution spectra give proof of this, showing a medium Raman band at  $386\text{ cm}^{-1}$  ( $\text{CCl}_4$ ), a weak infrared band at ca.  $306\text{ cm}^{-1}$  (*n*-heptane), and coincident IR (*n*-heptane)/Raman ( $\text{CH}_3\text{CN}$ ) bands at  $278\text{ cm}^{-1}$ . The medium IR absorption at  $345\text{ cm}^{-1}$  both in solution and in solid state, with a weak Raman counterpart at ca.  $347\text{ cm}^{-1}$  ( $\text{CCl}_4$ ), is presumably a Ni-C-O mode, as are the bands between  $650$  and  $400\text{ cm}^{-1}$ . Finally, the medium-weak Raman bands at  $222$  and  $247\text{ cm}^{-1}$  ( $248\text{ cm}^{-1}$  in  $\text{CH}_3\text{CN}$  solution) are presumably Cp-Ni bending modes.

**(D) Complexes of the Type CpM.** Analysis of the Raman spectrum of CpK is complicated by a fluorescent background, but no significant peaks seem to be present. In contrast, CpLi

(28) Oxtun, I. A. *J. Mol. Struct.* **1982**, 78, 77.

(29) Mitschler, A.; Rees, B.; Lehmann, M. S. *J. Am. Chem. Soc.* **1978**, 3390.

(30) Byers, L. R.; Dahl, L. F. *Inorg. Chem.* **1980**, 19, 680.

(27) Adams, R. D.; Collins, D. M.; Cotton, F. A. *Inorg. Chem.* **1974**, 13, 1086.

shows a strong Raman band at  $195\text{ cm}^{-1}$ , and its intensity and frequency unequivocally point to its assignment as a  $\nu(\text{Cp-Li})$  mode. CpTi has similar behavior: two weak but clear infrared and Raman bands, nearly coincident at ca.  $180\text{ cm}^{-1}$ , suggest a similar assignment; moreover, two weak infrared features at  $376$  and  $474\text{ cm}^{-1}$  are evident, which can tentatively be assigned to the  $e_1$  ring tilt and to the  $e_2$  ring deformation modes, respectively. So metal-ring interaction is confirmed. Of the compounds we have studied, the simple ionic model only applies to CpK.

### Discussion

Organometallic compounds are in general complex molecules, and an adequate vibrational treatment, i.e., a normal coordinate analysis and a force constant calculation, is a difficult problem. The frequencies are complex functions of atomic masses, force constants, and molecular geometry, and the number of observables is usually less than the number of unknowns. In practice, the spectra are sometimes simpler than expected, because of the weakness of some kinematic coupling. That is, the vibrations are sufficiently localized to treat a particular internal coordinate, like bond stretching, angle bending, and so on, on the basis of local symmetry, the symmetry of a single M-L unit. This is the case of the cyclopentadienyl ligand bonded to a metal center, as the analysis presented in this paper has shown. The negligible coupling between vibrational modes of different atomic character allows their separate treatment, and such a separate treatment is the basis of the following discussion.

**(1) C-H Stretching Vibrations.** These vibrational modes give rise to weak or medium infrared bands and to strong Raman bands with a typical pattern. Moreover, they appear to be more sensitive than any other modes to intra- or intermolecular effects, such as the variations in coordination between M and Cp, to ring deformations, or to intracrystal couplings. The frequency values lie in a narrow range, a statement particularly true for the most prominent feature, that associated with the symmetric mode. This range is  $3105 \pm 5\text{ cm}^{-1}$  for metallocene complexes and  $3125 \pm 5\text{ cm}^{-1}$  for cyclopentadienylmetal carbonyls. The difference is surely significant and may be ascribed to the well-known electron withdrawing effect of the CO groups. This effect can be transmitted *via* the metal to the ring, decreasing the negative charge on carbon atoms and reinforcing the C-H bonds. In accord with this interpretation, systems close to the ionic model limit  $[\text{Cp}^-][\text{M}^+]$ , where the negative charge on the  $\text{C}_5$  ring is greatest, show the lowest  $\nu(\text{CH})$  values ( $\leq 3090\text{ cm}^{-1}$ ).

**(2) C-C Stretching Vibrations.** The ring breathing mode is the most prominent band in the Raman spectrum of all of the compounds. Because of its intensity and frequency ( $1105 \pm 10\text{ cm}^{-1}$ ), it can be considered the most evident Cp group frequency. Apparently, this mode, along with the other  $\nu(\text{C-C})$  modes, does not show the sensitivity of the  $\nu(\text{C-H})$  modes to the metal-ring interaction. Rather it is sensitive to the carbon-carbon distance. The homologous series of the metallocene complexes follow a clear trend; the average C-C length varies roughly inversely with the frequency of the ring breathing mode, as Figure 9 shows. This behavior should not be overemphasized, because the C-C distances in any one molecule may differ, but it is not without significance. It seems that the symmetric expansion of the ring compensates in some way for the individual distance variations. A similar behavior has been reported for the model systems  $\text{Cp}_2\text{Fe}$ , CpLi, and  $[\text{Cp}^-]$ , where the C-C force constant increases in that order, indicating both an increase of the bond order and a decrease of the bond length.<sup>6</sup>

**(3) C-H Bending Vibrations.** The in-plane bending modes do not show any characteristic variations. The  $e_1$  (at  $1005 \pm 5$

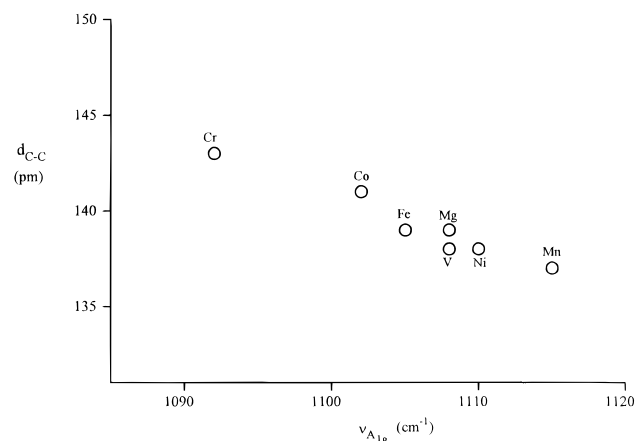


**Figure 9.** Average C-C distance vs frequency of the ring breathing mode for metallocene complexes.

$\text{cm}^{-1}$ ) has a stronger infrared than Raman intensity; the  $e_2$  (at  $1060 \pm 10\text{ cm}^{-1}$ ) shows the opposite pattern (Figure 1). The a-type mode is usually both IR and Raman inactive and can only sometimes be observed at ca.  $1200\text{ cm}^{-1}$ .

Much more interesting are the out-of-plane vibrations, one of which, the a-type, gives rise to the strongest infrared band in all of the complexes. This mode shows the largest frequency changes of all the intraring vibrations and has been the subject of some controversy. Two mechanisms have been invoked to explain the changes, a strong coupling with the Cp-M stretching modes or variations in electronic effects in the ring.<sup>4</sup> The former hypothesis points to the upward frequency shift of the covalent compounds with respect to the ionic  $[\text{Cp}^-][\text{M}^+]$  compounds: this shift was used as a measure of the covalency of the bond.<sup>3</sup> A normal coordinate analysis supported the hypothesis:<sup>31</sup> the same harmonic force field used for  $[\text{Cp}^-]$  fits the frequency values of  $\text{Cp}_2\text{Fe}$ , provided that appropriate kinematic coupling elements in the  $\mathbf{G}$  matrix are introduced. On the other hand, the use of different force field sets for  $[\text{Cp}^-]$  and  $\text{Cp}_2\text{Fe}$  give an equally good fit to the data,<sup>6</sup> indicating that the different frequencies arise from different force constant values, which in turn are due to different interactions between the (bonding) hydrogen 1s orbitals and the  $\pi^*$  orbital of the ring. That is, good fits in NCA are not *per se* a proof of validity; a better way forward is perhaps to refer to the chemical properties of the complexes or to make detailed comparisons of spectra. This latter approach leads us to favor the second hypothesis, that variations in electronic effects dominate trends in a-type CH bending frequency. For example, if the frequency values of the  $\gamma(\text{C-H})$  modes are taken to be rough measures of the covalency of the Cp-M bond, it is difficult to accept the consequent conclusion that  $[\text{Cp}_2\text{Fe}^+]$  and  $[\text{Cp}_2\text{Co}^+]$  are more covalent than  $\text{Cp}_2\text{Fe}$  or  $\text{Cp}_2\text{Co}$ , respectively, or, among the dimers, that  $\text{Cp}_2\text{Ni}_2(\text{CO})_2$  is less covalent than any other we have studied. Moreover, if the coupling between  $\gamma(\text{C-H})$  and  $\nu(\text{Cp-M})$  dominates the  $\gamma(\text{C-H})$  frequency shift, in the metallocene series we would expect similar coupling effect to be shown between appropriate pairs such as the two  $a_{1g}$  modes 2 and 4 compared with the two  $a_{2u}$  modes 9 and 11. It is hardly credible that the result of  $\gamma(\text{C-H}) - \nu(\text{Cp-M})$  coupling leads, for every compound, to very different values of  $\nu_4$  and  $\nu_{11}$  but to nearly identical values for  $\nu_2$  and  $\nu_9$  (cf. Tables 3 and 4).

Closer inspection of the frequency values of the three  $\gamma(\text{C-H})$  modes shows a surprising constant ratio  $\nu(a):\nu(e_1):\nu(e_2) = 1:\cong 1.03:\cong 1.1$ , a pattern which strongly suggests the

(31) Brunvoll, J.; Cyvin, S. J.; Schäfer, L. *J. Organomet. Chem.* **1971**, *27*, 107.



**Table 3.** Average<sup>a</sup> Experimental Frequencies (cm<sup>-1</sup>) of the Out-of-Plane C–H Bending Modes and Calculated Force Constants (10<sup>21</sup> (N·m)/rad)

complex	av freq at given mode <sup>b</sup>			
	a <sub>1</sub>	e <sub>1</sub>	e <sub>2</sub>	f <sub>γ</sub>
Cp <sub>2</sub> Mg	759	785	889	279
Cp <sub>2</sub> V	776	800	895	304
Cp <sub>2</sub> Cr	769	830	865	300
Cp <sub>2</sub> Mn	767		865	296
Cp <sub>2</sub> Fe	817	843	894	330
[Cp <sub>2</sub> Fe <sup>+</sup> ][I <sub>3</sub> <sup>-</sup> ]	850	876	930	362
Cp <sub>2</sub> Co	782	832	885	305
[Cp <sub>2</sub> Co <sup>+</sup> ][Br <sub>3</sub> <sup>-</sup> ]	863	895	941	371
Cp <sub>2</sub> Ni	771	793	842	291
CpMn(CO) <sub>3</sub>	835	849	940	347
CpRe(CO) <sub>3</sub>	826	843	932	341
CpFe(CO) <sub>2</sub> Cl	842	875		360
CpFe(CO) <sub>2</sub> Br	843	877		361
CpFe(CO) <sub>2</sub> I	844			360
Cp <sub>2</sub> Mo <sub>2</sub> (CO) <sub>6</sub>	824	844	912	336
Cp <sub>2</sub> W <sub>2</sub> (CO) <sub>6</sub>	832	844	914	339
Cp <sub>2</sub> Fe <sub>2</sub> (CO) <sub>4</sub> cis	825	847	880	332
Cp <sub>2</sub> Fe <sub>2</sub> (CO) <sub>4</sub> trans	826	832	875	330
Cp <sub>2</sub> Ni <sub>2</sub> (CO) <sub>6</sub>	774	806	836	295
CpLi	745	754		261
CpK	703	715		233
CpTl	732	748		252

<sup>a</sup> The average is of infrared and Raman absorptions. <sup>b</sup> The numbers in italics refer to a poor fit between experimental and calculated values (see text).

**Table 4.** Metal–Ring Stretching Force Constant and M–C Bond Distance of M–(η<sup>5</sup>-C<sub>5</sub>H<sub>5</sub>) Complexes

complex	f <sub>M</sub> (N/m)	k <sub>M</sub> (N/m)	d(M–C) <sup>a</sup> (pm)	ref <sup>b</sup>
Cp <sub>2</sub> Mg	125	39	230.4	33
Cp <sub>2</sub> V	202	45	224.5	34
Cp <sub>2</sub> Cr	215	88	216.9	34
Cp <sub>2</sub> Mn	192		241.1	21
Cp <sub>2</sub> Fe	316	53	203.3	35
[Cp <sub>2</sub> Fe <sup>+</sup> ][I <sub>3</sub> <sup>-</sup> ]	290	94	204.7	36
Cp <sub>2</sub> Co	221	71	209.6	37
[Cp <sub>2</sub> Co <sup>+</sup> ][Br <sub>3</sub> <sup>-</sup> ]	337	78	206.6	38
Cp <sub>2</sub> Ni	198	48	216.4	39
CpMn(CO) <sub>3</sub>	221		212.4	40
CpRe(CO) <sub>3</sub>	309		228.4	41
CpFe(CO) <sub>2</sub> Cl	222		207	42
Cp <sub>2</sub> Mo <sub>2</sub> (CO) <sub>6</sub>	256		234	27
Cp <sub>2</sub> W <sub>2</sub> (CO) <sub>6</sub>	306		234	27
Cp <sub>2</sub> Fe <sub>2</sub> (CO) <sub>4</sub> trans	229		211	29
Cp <sub>2</sub> Ni <sub>2</sub> (CO) <sub>6</sub>	276		211	30
CpLi	140		231.8	43
CpTl	104		271	44

<sup>a</sup> Average value. <sup>b</sup> Structural data.

validity of a local force field restricted to the out-of-plane vibrations with negligible interference of other vibrational modes. The values of the square root of the corresponding **G** matrix elements<sup>2,32</sup> are 1:1.12:1.43; the ratios are greater, but

the order is the same. So, appropriate **F** matrix elements may be chosen in order to modulate the **G** ratio and to fit the experimental ratio. No doubt there are many ways of doing this, but a very simple equation for the **F** matrix elements is

$$F(a) = f_{\gamma} + 2k_{\gamma}$$

$$F(e_1) = f_{\gamma} + 2 \cos(72^{\circ})k_{\gamma}$$

$$F(e_2) = f_{\gamma} + 2 \cos(144^{\circ})k_{\gamma}$$

where two variables only are considered,  $f_{\gamma}$ , the main force constant, and  $k_{\gamma}$ , the interaction constant between two vicinal out-of-plane CH bending internal coordinates; the other interaction between nonvicinal CH bending coordinates is neglected. Using the same  $k_{\gamma}$  value for all of the complexes ( $47 \times 10^{21}$  (N·m)/rad has been chosen, as the average of the values obtained by separate fittings),  $f_{\gamma}$  values were calculated. Despite the gross approximation involved, the fitting is satisfactory—most of the calculated  $\nu$  values are within 2% of the experimental ones (Table 3). Clearly this agreement cannot be considered proof of the correctness of the above equation. More complete force fields should give (and have given) much better fits. It is noteworthy, however, that such a simple assumption (it is probably the simplest of all) gives rise to an acceptable fitting for a large number of different complexes. In normal coordinate analysis of complex molecules, any level of precision can be reached provided that the basis set is large enough. Therefore, the intrinsic value of a model may perhaps best be judged against the criterion “the simplest, the best”, which is the strategy presented here.

All of the observations reported in this work point to the minor role played by coupling between the M–Cp stretching modes and the out-of-plane bending frequencies. The values of the force constants, which, of course, parallel those of the frequencies (Table 3), could be taken as approximate measure of the difficulty of moving the hydrogen atoms towards the C<sub>5</sub> ring. Ziegler,<sup>6</sup> comparing Cp<sub>2</sub>Fe and [Cp<sup>-</sup>], ascribed this effect to an energy increase of the  $\pi^*$  orbital of the ring in Cp<sub>2</sub>Fe with respect to [Cp<sup>-</sup>], leading to a decrease in the stabilizing interaction between these orbitals and the 1s H orbitals. Without excluding this point, the  $f_{\gamma}$  values suggest another effect, the electrostatic interaction between the small residual positive charge on the H atoms and the variable charge on the ring. It is surely not without significance that the highest  $f_{\gamma}$  values are shown by the metallocinium cations and by the complexes where electron withdrawing groups like CO or halogen atoms are bonded to the metal atom, whereas the lowest  $f_{\gamma}$  values are shown by complexes closer to the ionic model [Cp<sup>-</sup>][M<sup>+</sup>]. Increased positive charge (or decreased negative charge) on the ring increases the H-ring repulsion (or decreases the H-ring attraction), increasing the force constant.

**(4) Cp–M Stretching Vibrations.** The assignment of the Cp–M stretching modes is straightforward, as described before, and allows the calculation of an approximate value for the Cp–M stretch force constant  $f_M$  with a simple three-body model for metallocenes or a two-body model for complexes with a CpM unit. These values are reported in Table 4. Haaland<sup>45</sup> considered  $f_M$  to be one of the important parameters to describe the character of the Cp–M bond in metallocenes or, more generally, the stability of Cp<sub>2</sub>M molecules. Even though this suggestion was based on incomplete and, sometimes incorrect,

(32) Fateley, W. G.; Curnutte, B.; Lippincott, E. R. *J. Chem. Phys.* **1957**, *26*, 1471.

(33) Bänder, W.; Weiss, E. *J. Organomet. Chem.* **1975**, *92*, 1.

(34) Gard, E.; Haaland, A.; Novak, D. P. *J. Organomet. Chem.* **1975**, *88*, 181.

(35) Takusagawa, F.; Koetzle, T. F. *Acta Crystallogr.* **1979**, *B35*, 1074.

(36) Bernstein, T.; Herbstein, F. H. *Acta Crystallogr.* **1979**, *B24*, 1640.

(37) Bänder, W.; Weiss, E. *J. Organomet. Chem.* **1975**, *92*, 65.

(38) Bockman, T. M.; Kochi, J. K. *J. Am. Chem. Soc.* **1989**, *111*, 4669.

(39) Seiler, P.; Dunitz, J. D. *Acta Crystallogr.* **1979**, *B36*, 2255.

(40) Fitzpatrick, P. J.; Le Page, Y.; Sedman, J.; Butler, I. S. *Inorg. Chem.* **1981**, *20*, 2852.

(41) Fitzpatrick, P. J.; Le Page, Y.; Butler, I. S. *Acta Crystallogr.* **1979**, *B37*, 1052.

(42) Jens, V. K. J.; Weiss, E. *Acta Crystallogr.* **1979**, *C41*, 895.

(43) Harder, S.; Prosen, M. H. *Angew. Chem., Int. Ed. Engl.* **1994**, *33*, 1744.

(44) Tyler, J. K.; Cox, A. P.; Sheridan, J. *Nature* **1959**, *183*, 1182.

(45) Haaland, A. *Acc. Chem. Res.* **1979**, *12*, 415.

data, we believe that the basic idea is correct. For example,  $[\text{Cp}_2\text{Fe}^+]$  with one bonding electron less than  $\text{Cp}_2\text{Fe}$  is characterized by a lower  $f_M$  value, whereas the opposite is true for the  $[\text{Cp}_2\text{Co}^+]/\text{Cp}_2\text{Co}$  pair, the first has one less antibonding electron with respect to the second. Moreover, the low value for  $\text{Cp}_2\text{Mn}$  reflects the destabilizing high-spin electronic configuration.<sup>1,45</sup>

The complexes traditionally taken as ionic require some comment. On the above criterion  $\text{CpLi}$  is nearly ionic: its  $f_M$  value is ca. 5–10% of the average value of a typical covalent complexes.  $\text{CpTl}$  and, surprisingly,  $\text{Cp}_2\text{Mg}$  show more covalent character. The low oxidation state and the availability of 6p and 6d orbitals for Tl are surely conducive to a significant covalency in the bond. For magnesiocene, the nature of the bonding was long in dispute, chemical, structural, and spectroscopic investigations often pointing in different directions.<sup>46</sup> The  $f_M$  value suggests a bond intermediate between ionic and covalent limits.

One typical spectroscopic/structural relationship is that between stretch force constant and bond length. It was recognized for a few metallocenes and is now evident for several  $\text{Cp-M}$  complexes that  $f_M$  roughly decreases as the metal–ring bond distance increases. Figure 10 shows this trend. To minimize the effect of the atomic size,  $f_M$  is reported against the difference between the  $\text{Cp-M}$  distance and the M covalent radius. The scatter of the points reflects both the approximations in the  $f_M$  calculation and the uncertainties in the bond length and the metal radii. However, the trend is clear. Note the position of  $\text{Cp}_2\text{Mg}$  and, especially, of  $\text{CpLi}$ , which are indicative

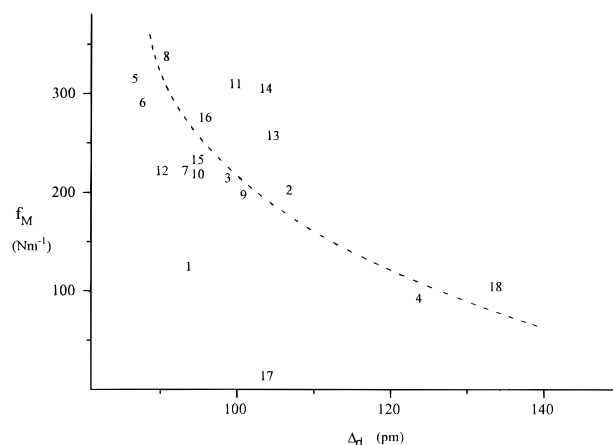


**Figure 10.** Metal–ring stretching force constant vs the difference between the metal–ring distance and the metal covalent radius. See Table 4 for the numbers.

of the partial (Mg), or of the prevailing (Li), ionic character of the bond, as suggested above.

**Acknowledgment.** Financial supports from CNR (progetto bilaterale di ricerca for P.L.S. and S.F.A.K.) and from MURST (40% funding to R.R. and E.D.) are gratefully acknowledged.

**Supporting Information Available:** Figures of the IR and Raman spectra of  $\text{CpFe}(\text{CO})_2\text{Cl}$  (Figure S1), of  $\text{trans-Cp}_2\text{Fe}_2(\text{CO})_4$  in solid state (Figure S2) and in solution (Figure S3) and of  $\text{Cp}_2\text{Ni}_2(\text{CO})_2$  (Figure S4) (4 pages). Ordering information is given on any current masthead page.

IC960545N

(46) Pinkus, A. G. *J. Chem. Educ.* **1978**, 704.